First Principles Investigation of Lithium Polysulfide Structure and Behavior in Solution

Ethan P. Kamphaus and Perla B. Balbuena*
Department of Chemical Engineering, Texas A&M University,
College Station, TX 77843
***balbuena@tamu.edu**

Abstract

The Lithium-Sulfur battery is a promising next generation energy storage technology that could meet the demands of modern society with a theoretical specific energy near 2500 W h kg^{-1}. However, this battery chemistry faces unique problems such as the parasitic polysulfide shuttle reaction which hinders battery performance severely. This shuttle phenomenon is caused by solubilities of intermediate reaction products in the electrolyte during the reduction chemistry of the battery. With molecular simulation and computational chemistry tools, we studied the thermodynamics, solvation structure, and dynamics of the long-chain lithium polysulfide species Li_2S_6 and Li_2S_8 in dimethoxyethane and 1,3-dioxolane to gain a deeper fundamental understanding of this process. We determined the structure of the 1st solvation shell for Li^+ as well as those of Li_2S_6, Li_2S_8 closed and Li_2S_8 linear in pure solvents and solvents with extra Li^+ added. The lithium polysulfide species were found not to favor dissociation and would most likely exist as fully lithiated species in solution.

Introduction

From electric vehicle applications and storage of non-grid based energy storage to consumer electronics, batteries are a critical and important technology. Demand for advanced energy storage in our modern society is significant thanks to a wide variety of applications and technologies [1-3] .Currently, the lithium ion battery (LiB) is used to meet this demand and is being used in these applications. As more research is conducted, the LiB battery continues to improve. Predictions have placed the maximum specific energy of LiB's up to 387 Wh/kg. Unfortunately, this energy density is not high enough for many applications. For instance, a battery needs to have a theoretical specific energy of 600 Wh/kg to be useful for electric vehicles with a range of 300 miles or greater [2, 4-5]. Any large improvement in specific energy density over the LiB would be greatly beneficial to many of the technologies used every day.

One battery that meets these requirements is the Lithium-Sulfur (Li-S) battery with a theoretical specific energy of around 2500 W h kg^{-1} [6]. Using sulfur based cathode chemistry has other advantages as well like reduced cost, safety, and low toxicity [1-3, 7]. Though the Li-S battery may seem highly promising; the system faces many difficult problems. Usually, Li-S batteries struggle from capacity fading and mediocre cycle performance as well as poor stability of anode and active material loss on the cathode [7-8]. One of the largest problems facing the current Li-S

battery is the polysulfide shuttle effect. This shuttle phenomenon leads to significant self-discharge and low coulombic efficiency, which severely hampers battery performance [1, 7]. This parasitic process is a result of the solubility of intermediate polysulfide species (Li_2S_n) formed in the reduction of elemental sulfur S_8 into the final desired reduction product Li_2S. When the polysulfide species dissolves in the electrolyte, it is moved from the cathode where the reduction takes place to the Li metal anode where the species finishes its reduction and becomes trapped as insoluble Li_2S [4, 6, 9-10]. The polysulfide shuttle effect is a very large problem that the Li-S battery must overcome to become commercially viable [1, 10-11].

Countering the polysulfide shuttle effect has been approached with different methods from both computational and experimental studies. Kang et al covered many of the different methods and ideas for stopping the shuttle effect in their recent review paper [8]. Many studies have investigated trapping polysulfide species on the cathode with additives or unique cathode architecture [12-16]. Some authors have researched engineering the solid electrolyte interphase (SEI) on the anode to alleviate the shuttle effect by preventing the reduction on the anode [7]. Others have focused on the effect of the electrolyte composition and performance [9, 17-18]. Since the fundamental reason behind the shuttle phenomenon is the solubility of polysulfide species in the electrolyte, investigating and engineering the Li-S electrolyte will be very important to solving the shuttle problem [1, 3, 18-19].

The current Li-S battery electrolyte usually consists of a solvent, lithium salts, and additives. The solvents main role is to ensure the diffusion of Li^+ ions through the battery. If a solvent or an electrolyte has poor ionic conductivity, it will harm battery performance [10, 20]. Many different electrolyte solvents have been studied like THF [21-22] , Acetonitrile [23-24] ,Dimethoxyethane (DME) [25] and 1,3 dioxolane (DOL) [26] with different advantages and disadvantages. The lithium salts like LiTFSI and LiFSI are used to help form favorable SEI on the Li metal anode [2, 11, 27-28] . Additives like $LiNO_3$ are also used in Li-S battery since they increase the electrochemical performance [13, 28-29] . Considering the electrolyte during electrochemical cycling, then the solution will also contain Li^+ ions (both from the salt and from cycling) and polysulfides due to the shuttle effect [1, 7]

Experimental studies have investigated the speciation of polysulfide species in the electrolyte [30-31]. UV-Vis spectroscopy has been utilized to determine the chain length of the polysulfide species that are formed on the cathode and dissolved in the electrolyte. These speciation studies have found that the longer chain polysulfide species are more soluble in the electrolyte [19, 30-31]. X-ray absorption and Raman spectroscopy have also been used for similar purposes [11, 29, 32-33].

Due to the spectroscopic evidence, much is known regarding the length of polysulfide species in the electrolyte. However, there are many questions that have not been answered and many assumptions have been made. For instance, the molecular nature of the polysulfide shuttle phenomenon seems to still be unknown. Some work refers to the polysulfide anion becoming solubilized in the electrolyte and diffusing across the battery to cause the shuttle effect [6, 8, 19, 34-35].

In contrast, other work refers to the polysulfide species in solution as lithiated neutral species [4, 17, 23, 31]. This indicates that there is a lack of fundamental understanding of exactly how the polysulfide behaves in the bulk electrolyte.

Computational studies have reported aspects of Li^+ ion solvation and the polysulfide shuttle effect[17, 20, 36-37]. These studies calculated lithium polysulfide solubilities and structures in different solvents but didn't explore in depth the structure of the polysulfide anions or the energetics and thermodynamics of dissociation in solution. Prendergast et. al. explored the structure and solubility of lithium polysulfides with explicit solvent but they didn't examine the dissociation behavior. Persson et. al. also examined the structure of lithium polysulfides in solution with special focus on cluster formation but did not investigate dissociation dynamics. Our goal is to explore the behavior and state of long chained polysulfide species in an electrolyte as an overall neutral charge fully lithiated species and as a free anion using first principles computational methods. We focus specifically on the dissociation of the lithium polysulfides since their degree of lithiation in the bulk electrolyte is important for mass transport which is critical to the polysulfide shuttle phenomenon. Both *ab initio* molecular dynamics (AIMD) and free energy quantum chemical calculations are employed to characterize the behavior, structure, and thermodynamics of the polysulfides (PSs) in solution.With greater fundamental understanding of one of the most critical problems of the Li-S battery, solutions can be discovered and approached more easily.

.

Computational Methods

Ab Initio Molecular Dynamics

The dynamics of the different polysulfide species were investigated with AIMD implemented with the Vienna *Ab Initio* Simulation Package (VASP) [38-40]. Dynamics were explored with a NVT ensemble at 300 K. Hydrogen masses were changed to Tritium to allow for 1 fs time step and the Nose thermostat was used to control temperature oscillations with 0.5 used as the Nose mass parameter. The electronic calculations were carried out for the dynamics with the projector augmented wave (PAW) pseudopotentials from the VASP libraries were used to calculate electron-ion interactions [41-42], and the Perdew-Burke-Ernzerhof generalized gradient approximation (PBE-GGA) for the exchange-correlation functional [43]. A plane wave basis set was used with an energy cutoff of 400 eV and Gaussian smearing with a width of 0.05 eV was implemented for partial occupancies of wave functions. A 2x2x2 Monkhorst-Pack k point grid was used for surface Brillouin zone integration [44].

PS species were placed in the middle of 15 x 10 x 10 Å cells that were created with Materials Studio [45]Solvent molecules were packed around the PSs randomly based on the density of the

solvent (0.87 g/cm^3 for DME and 1.06 g/cm^3 for DOL) with a built-in amorphous packing tool to generate a PS surrounded by solvent molecules representing the liquid electrolyte.

Although usually the electrolyte contains a mixture of solvents along with Li-salts and other additives, in our study the Li-S battery electrolyte was simplified by removing the presence of Li-salts and by using either pure (DME) or pure (DOL). Therefore, the focus was on the interactions between just the polysulfide species and the solvent molecules. Three different PS species were tested: Li_2S_6 and two different conformations of Li_2S_8. .The Li_2S_8 conformations were based on the preferred structure of the polysulfide with and without Li^+ ions. The Li_2S_8 closed structure is slightly preferred in neutral state whereas the Li_2S_8 linear is preferred in dianion state because that conformation allows charged ends of the polysulfide to be separated by a larger distance [4]. Only long chain PS species were examined since they are known to be more soluble in the electrolyte versus shorter chains [19, 30-31]. Radical sulfur species were not explored in this work. The structures used to build the AIMD models were optimized in prior work and are shown in Figure S1 in the supporting information [36].

Before running AIMD on the initial configurations, classical molecular dynamics was used to quickly relax the overall energy of the system. The universal force field[46] was used with a conjugate gradient algorithm within Material's Studio built in package [45]. Then the AIMD simulations were carried out for at least 15 ps in order to ensure that equilibrium was reached and that the structures would represent a solution of the same composition. Bader charge analysis was used to estimate the partial charges of different atoms in the dynamic simulations [47-49]. Radial distribution functions (RDF) to determine structure of interactions in the liquid electrolyte were evaluated from the AIMD trajectories using Visual Molecular Dynamics (VMD) [50].

Thermodynamics of Polysulfide Solvation

The solvation structures, energetics and thermodynamics were characterized with Gaussian 09 (G09) [51].Free energies were calculated from geometry optimization simulations by computing electronic, translational, vibrational, and rotational contributions using the equations from statistical thermodynamics[52]. Hybrid PBE exchange correlation functional [53] was used with the 6-311++G(d,p) basis set [54]. PS structures were examined with a cluster–continuum model where the first solvation shell was calculated explicitly while a polarized continuum model (SMD) [55] was used to represent the rest of the liquid electrolyte. This functional was chosen over B3LYP and standard PCM since hybrid PBE gave more realistic thermodynamically favored first solvation shell coordination numbers (Table S2). The cluster–continuum model has been shown to increase the accuracy of calculations and provide more insight since solvent molecules beyond the first shell are actually modeled [20, 56]. Basis set superposition error (BSSE) was not calculated for this work since the counterpoise method in Gaussian cannot be used with implicit solvation methods. Reported BSSE in similar systems was found to be < 3 kcal/mol and will not have a impact on our results Configurations for these calculations were based on structures observed

during the AIMD simulations. In these simulations, the behavior of solvent interactions with Li^+ and lithium polysulfides were observed. Based on these observations, all possible simple configurations of the 1st solvation shell we able to be constructed and simulated.

Results and Discussion

The behavior, structure, and state of dissolved PS in the electrolyte will most heavily depend on the amount of Li^+ that are coordinating the anionic PS species. Three PS states were examined: overall neutral species coordinated with two Li^+ ions, overall -1 charge coordinated with one Li^+ ion, and overall -2 charge with no coordinated Li^+ ions.

Characterization of Li_2S_6, Li_2S_8 Closed, Li_2S_8 Linear in Simple Electrolyte

Dynamics of Neutral Li_2 Polysulfide species

The dynamics of the PS species coordinated with two Li^+ ions were investigated first. Snapshots of the AIMD simulations after at least 15 ps are shown in Figure 1.

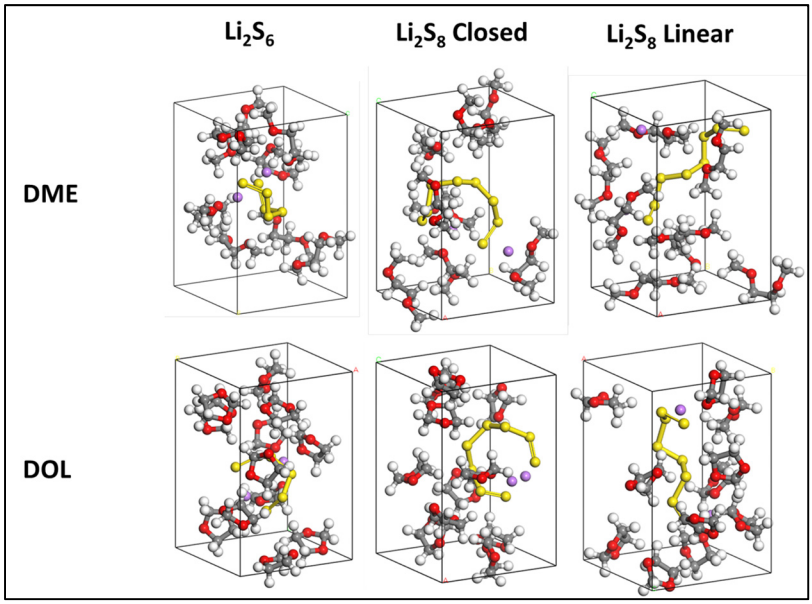

Figure 1: Snapshots taken of Li_2PS with DME/DOL systems after at least 15 ps of AIMD simulation time.

Several observations can be drawn from the dynamics of the PS species in solution throughout the AIMD simulation. One of the most important observations is that the only clear solvent-solute interactions are between the oxygen atoms from both solvents and the Li^+ ions from the PS species. This interaction is well known and expected. Many papers have been published about how different solvent molecules interact with Li^+ ions such as ethers and carbonates [3, 9, 14]. The interactions between different atom types within the system can be described and quantified by

radial distribution functions (RDF) between different species as shown in Figure 2 for the Li_2S_8 linear molecule. RDFs for the other species are reported in Figure S2.

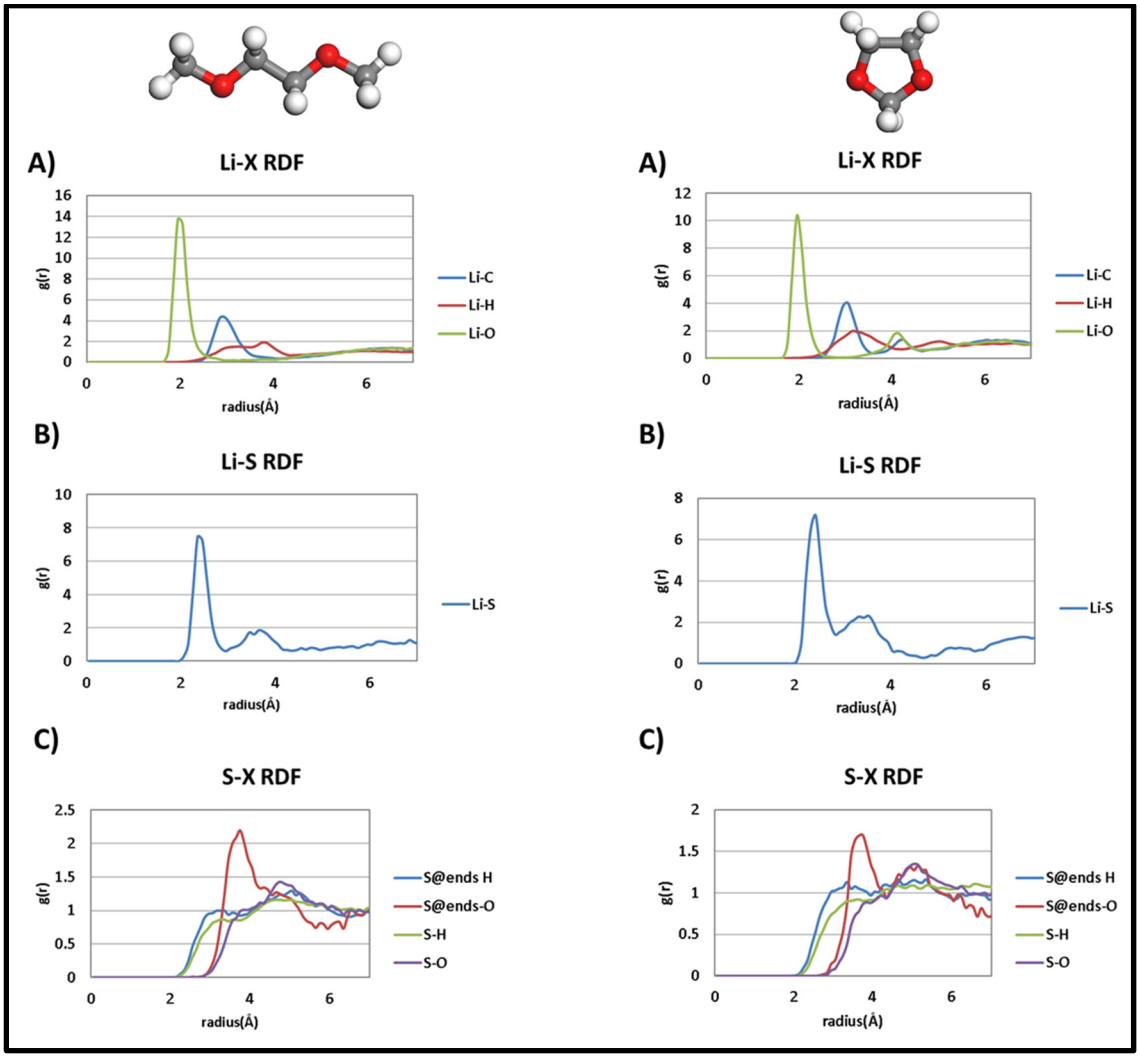

Figure 2: A) Li-X, B) Li-S and C) S-X Radial Distribution functions for Li_2S_8 linear with DME (left) and DOL (right) after at least 15 PS of AIMD

The RDFs between the PS species and solvents are all very similar with some slight differences. It is demonstrated by the Li-X RDFs that the Li^+ ions closely interact with both solvent molecules. The Li-O first peak is the closest to the Li^+ ion and the largest, which indicates that solvent coordination occurs via oxygen interactions with the ion and the peaks from the other atoms result from the structure of the solvent itself. The Li-O peaks are higher in DME for all the cases most likely due to the ability of DME to coordinate more than once per molecule since the solvent molecule can rearrange. DOL cannot rearrange to have both oxygens coordinate with Li^+ ions due to its cyclic structure.

The Li-S RDFs are similar but have slight differences due to the polysulfide's geometry. The presence of more than one peak and the size of that peak show that the Li^+ ions are closely bound to the PS throughout the dynamics. Solvent choice does not seem to affect these interactions greatly. This leads to the conclusion that the PS is always closely interacting with Li^+ ions for these simulations. In this simplified model for the electrolyte no evidence of the *spontaneous formation* of a PS anion (1 Li^+ coordinating) or dianion (no coordinating Li^+ ions) was observed.

The electronic distribution calculated with Bader partial charge analysis of the neutral Li_2S_6 and Li_2S_8 species are shown in Figure S3. The sulfur atoms at the end of each PS have a more negative charge than the intermediate S atoms in the chain, which are also negatively charged. The positively charged Li^+ ions closely interact with the sulfur atoms at the end of the PS species due their higher negative charge. Based on the charge analysis if the solvent had to coordinate the sulfur itself, the solvent molecule would solvate via the hydrogen atoms instead of the oxygen atom [9].

The RDFs for S-X for both the S atoms at the end and in the middle of the polysulfide were investigated to gain more understanding about how the solvent may interact with the sulfur itself. In all of the simulations, the interactions between the S atoms in the middle of the molecules with hydrogen and oxygen did not have any noticeable peaks, which indicate that the solvent molecules were not interacting with the sulfur atoms in any particular order.

In contrast, the RDF for the S-O and S-H interactions for the S atoms at the ends of the PS molecule do have clear peaks for both oxygen and hydrogen. The peak for hydrogen interactions is smaller than the peak for oxygen interactions, but the hydrogen peak is closer to the S atom. The peak from oxygen is due to interactions between the Li^+ and the end sulfur atoms since the Li^+ ion is closely bound to both the sulfur and the solvent molecules. This "transitive" coordination with the oxygen atoms explains why the peak is relatively strong but farther than expected for coordination. By this logic, the very small peak for hydrogen is also related to the Li^+ ion solvation. The solvent molecule may arrange itself while coordinating with Li^+ ions so that some of the hydrogen atoms are interacting with the more negatively charged sulfur atoms at the end of the PS species.

Thermodynamics of Solvation Structure for Neutral Li_2 Polysulfides

The dynamics of the PS species in solution provided insight into the molecular processes behind the PS state and structure. However, it is difficult to understand or interpret the dynamics without having an even more fundamental understanding of the system. Determining thermodynamically favorable solvation structures will break down the solvation dynamics into discrete solvation structures, provide greater fundamental insight, and allow for further calculations on the neutral Li_2 polysulfide species. Thus, additional first principles calculations were used to determine the energetics, geometries and therefore the thermodynamics of specific first shell solvation structures.

Before examining the Li_2S_6, Li_2S_8 closed, and Li_2S_8 linear structures, Li^+ ion solvation thermodynamics were studied for DME and DOL as shown in Figure 3. The structures that correspond to the various intermediate states shown in Figure 3 are in Figure S4 and Figure S5 respectively. Example results are shown for Li^+ with DME in Table 1. Results for DOL are shown in Table S3.

Table 1: ΔG of solvation (kcal/mol) for thermodynamically favored Li^+ DME structures obtained from Hybrid PBE/6-311++G(d,p)/SMD . All the structures are shown in Figures S4.

Number of solvent molecules							
1		**2**		**3**		**4**	
A--> B	-9.53	**B --> C**	-1.54	**C --> D**	0.38	**D --> F**	-11.63
A --> G	-22.47	**B --> E**	-27.31	**C --> F**	-11.25	**F --> J**	-5.19
		B --> G	-12.94	**C --> E**	-25.76	**J --> I**	-1.70
		G --> E	-14.36	**E --> F**	14.51		
		G --> H	-13.91	**E -- > J**	9.32		
				E --> H	0.46		
				H --> J	8.86		
				H --> I	7.16		

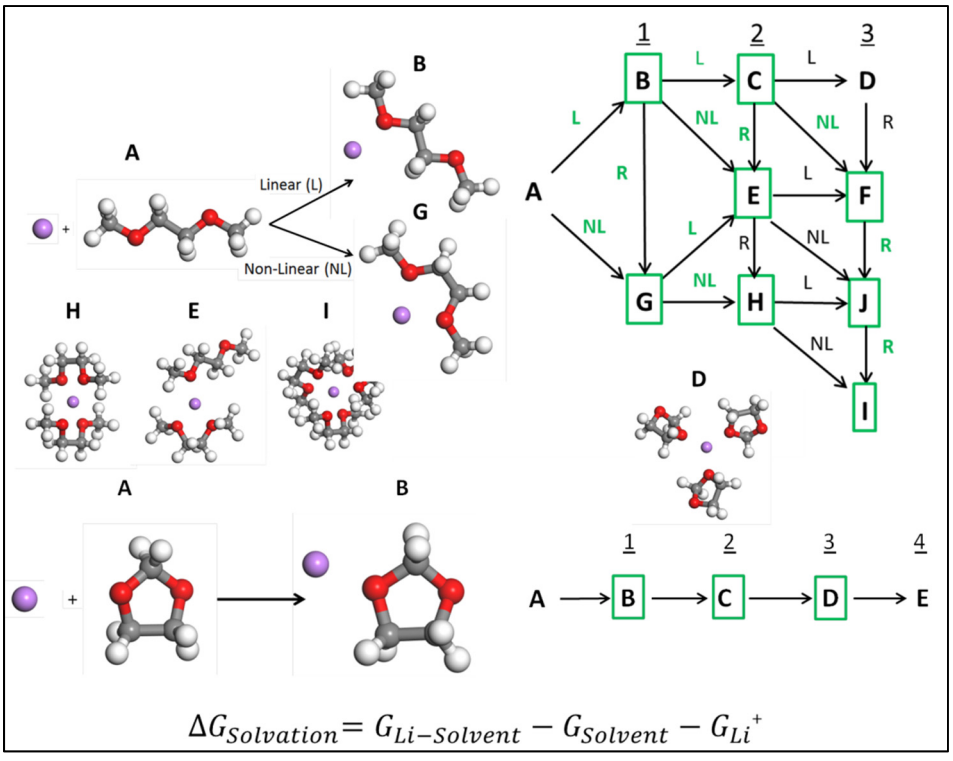

Figure 3: Thermodynamically favored solvation structure diagram for Li^+ ion with DME and DOL. Each letter represents a unique geometry of Li^+ ion with solvent molecules. All the structures are shown in Figures S4 and S5 for DME and DOL respectively. DME molecules were added in either their linear configuration (L) or nonlinear configuration (NL). Rearrangements (R) between linear and nonlinear DME configuration may also occur. DOL can only be added in one way. All letters surrounded by green boxes are favored thermodynamically. All letters highlighted in green are favorable solvent additions or rearrangements.

DOL has less possible solvation structures since it can only coordinate with Li^+ ions in one way due to its molecular structure. In contrast, a DME electrolyte has several possible solvation structures since it can coordinate with Li^+ ions in more than one way. The final *thermodynamically favored* solvation structures found for Li^+ are H, E, and I for DME and D for DOL. Thus, if given infinite time to establish equilibrium, a Li^+ ion in a pure solution of DME or DOL will eventually reach one of these favored structures for the first solvation shell. The expected coordination number for DOL is 3 and from 3 to 6 for DME. These numbers are similar to coordination structures reported for other solvents [57]. This analysis provides a starting point for creating the same type of solvation diagrams for the polysulfide species. Solvation diagrams with the thermodynamically favored structures identified are shown in Figure 4 for Li_2S_6 and Li_2S_8 Closed and Figure S6 for Li_2S_8 Linear in DME. The structures that correspond to intermediate states shown in these diagrams are displayed in Figure S7, Figure S8 and Figure S9. Solvation free energies for the thermodynamically favored solvation structures for Li_2S_6 DME are shown in Table 2.

Table 2: ΔG of solvation (kcal/mol) for thermodynamically favored Li_2S_6/DME solvation structures obtained from Hybrid PBE/6-311++G(d,p)/SMD

# of Solvent Molecules									
1		**2**		**3**		**4**		**5**	
A --> B	-3.68	**B --> K**	3.70	**K --> L**	-5.07	**L --> F**	12.92	**E --> F**	0.45
A --> N	-11.48	**B --> C**	-0.41	**K --> D**	0.89	**L --> D**	5.95	**E --> H**	1.01
		B --> I	-7.70	**K --> M**	-3.62	**D --> E**	6.51		
		B --> M	0.08	**C --> D**	4.99	**D --> F**	6.96		
		B --> N	-7.80	**C --> G**	1.60	**D --> G**	-3.38		
		N --> I	0.10	**C --> I**	-7.29	**G --> F**	10.35		
		N --> M	7.88	**I --> G**	8.90	**G --> H**	10.90		
		N --> O	-6.39	**I --> J**	4.69	**G --> J**	-4.20		
				I --> O	-6.49	**J --> H**	15.11		
				M --> G	1.12				
				M --> J	-3.09				
				O --> J	11.18				

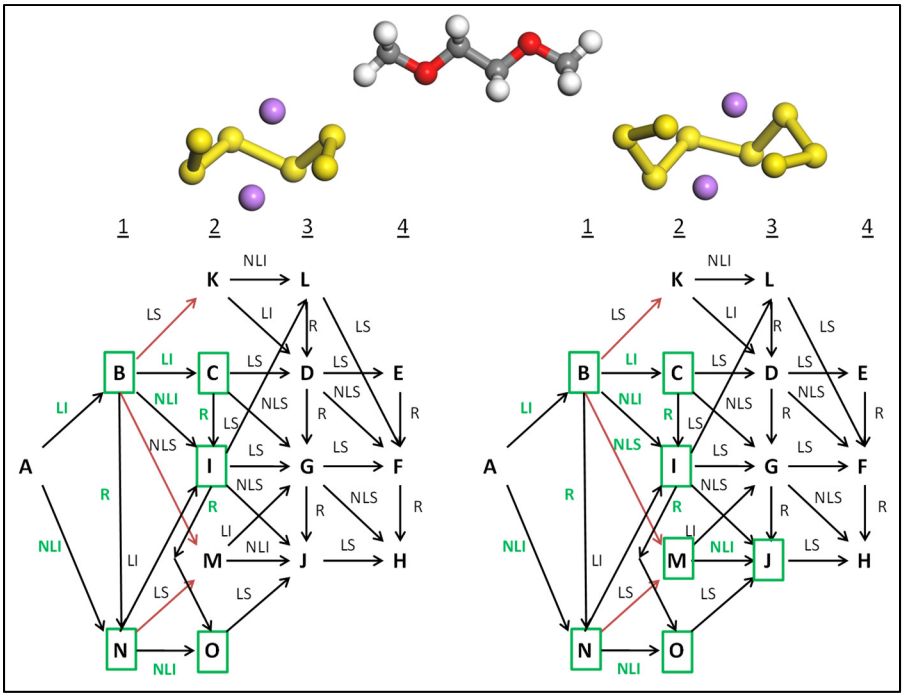

Figure 4: Thermodynamically favored solvation structure for Li_2S_6, and Li_2S_8-closed in DME. Each letter represents a unique geometry of PS with DME molecules. The numbers on top indicate the total number of DME molecules involved in solvation structure. All letters surrounded by green boxes are favored thermodynamically. All letters highlighted in green are favorable solvent additions. Red arrows represent "non-orderly" addition (adding solvent molecule to the same Li^+ consecutively). The labels over the arrows refer to order and type of solvent addition as follows: LI: linear initial (mono-coordinated Li^+); NL stands for nonlinear addition (Li^+ bi-coordinated to the same molecule). I, S and T stand for initial, secondary and tertiary additions of solvent molecules.

The solvation diagrams increase in complexity compared to just the Li^+ ion when the Li_2PS species are considered since there are now 2 Li^+ ions and the structures aren't exactly same as the case with just the ion since the S atoms and other solvent molecules create a steric shielding effect.

Both of the Li_2S_8 species have thermodynamically favored solvation structures that contain up to 3 DME molecules versus the Li_2S_6 molecule only had solvation structures with up to 2 DME molecules. The Li_2S_6 solvation structures were tighter due to the size of the polysulfide, which is most likely the reason for less DME coordination.

The same analysis of the solvation structures for the different polysulfide species with DOL are shown in Figure 5. The structures corresponding to the intermediate states shown in Figure 5 are found in Figure S10, S11, S12.

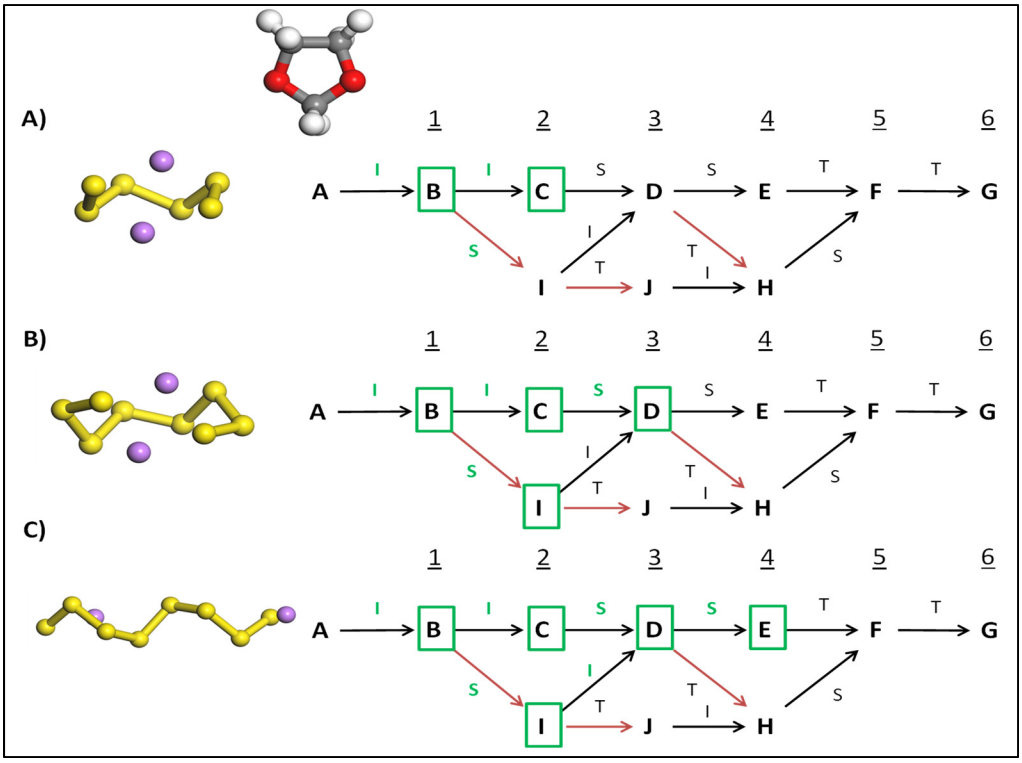

Figure 5: Thermodynamically favored solvation structure for A) Li_2S_6 B) Li_2S_8 closed C) Li_2S_8 Linear in DOL. Each letter represents a unique geometry of PS with DOL molecules. The numbers on top indicate the total number of DOL molecules involved in solvation structure. All letters surrounded by green boxes are favored thermodynamically. All letters highlighted in green are favorable solvent additions. Red arrows represent "non-orderly" addition (adding solvent molecule to the same Li^+ consecutively). I, S and T stand for initial, secondary and tertiary additions of solvent molecules.

Similar trends are found for the DOL electrolyte compared to the DME electrolyte. The longer PS species have thermodynamically favored solvation shells with more DOL molecules than the shorter chained Li_2S_6.

The solvation diagrams show what possibilities exist for the first solvation shell of Li_2S_6, Li_2S_8 closed and Li_2S_8 Linear with DME and DOL if given the requirements to establish equilibrium. In a real Li-S battery operation, any neutral Li_2PS species would be expected to follow the thermodynamically stable configurations when only considering PS and solvent interaction.

Dynamics + Thermodynamics

With a greater fundamental understanding of the polysulfide's preferred solvation state in the solution, the AIMD simulations were revisited to compare with the thermodynamic calculations. Figure 6 demonstrates this analysis for Li_2S_8 Linear with both DME and DOL. Other PS coordination over time is shown in Figure S13.

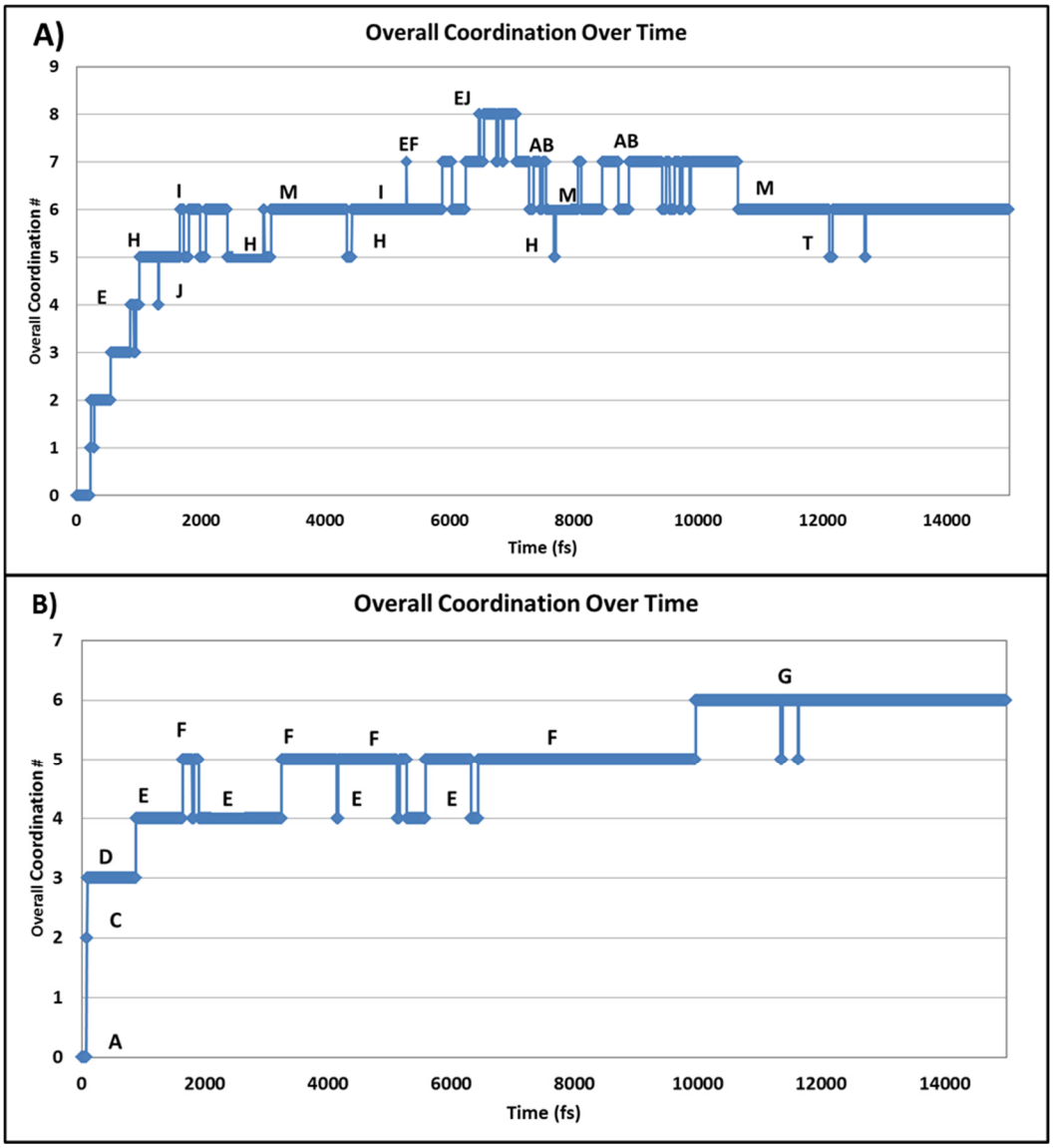

Figure 6: Overall coordination over 15 ps for AIMD Li_2S_8-Linear simulations in solution of: A) DME B) DOL The letters on each graph correspond to the thermodynamic solvation diagrams shown in Figure S6 and Figure 5-c for DME and DOL respectively. If a graph has two letters, then the solvation compares more to the Li^+ solvation and each letter stands for one of the structures on Figure 3.

There are several interesting observations that can be drawn from these graphs. First, there are several structures that appeared in the dynamics that were not predicted as thermodynamically favorable. For instance with the DOL simulations, structures F and G were not favorable (Figure 5) and for DME, structure H was not favored (Figure S6). Another observation for the DME system is the presence of structures EF and EJ. These structures were not predicted at all by the calculations for the PS species, but instead come from the calculations that only considered the Li^+ ion (a combination of E and F or E and J for the Li^+ solvation structure). The solvation

looked more like Li^+ solvation than Li_2PS solvation. Similar trends can be concluded from the other systems (Figure S13).

The differences between the dynamics simulations and the thermodynamic calculations could arise from a variety of reasons. Modeling the full electrolyte explicitly could change the first solvation shell some depending on how much the explicit solvent molecules would have a different effect than the implicit continuum model. Though the AIMD simulations use more solvent molecules, the static DFT calculations use a more accurate functional. Another potential explanation could be that those configurations are just long lived non-equilibrium structures that could arise in dynamic simulations but, Figure 6 shows that some of the non-thermodynamically predicted structures are quite long lived. The long lived structures shown in Figure 6 also demonstrate the dynamic equilibrium that the system has reached. Some changes may still occur but most structures are longer lived. Note that we do not claim that a global minimum has been achieved in the simulations. Sometimes systems may get trapped in local minima. However, considering the simulations results, we suggest that these local minima should be quite frequent.

The most reasonable explanation for the observed differences is that the Li^+ ions are slightly less bound or ordered in the dynamics simulations versus the thermodynamic calculations. The structures of the solvated Li_2PS species used in the thermodynamic calculations are quite similar to the structure of the Li_2PS species without solvent. The Li^+ ions are still tightly bound to the PS molecules though the more solvent molecules are coordinating the Li^+ ions the longer the Li^+-S ionic bond is. In the dynamics simulations, the Li^+ ions are found to still be bound to the polysulfides but less closely than observed in the thermodynamic analysis. The looser Li^+ ions are less sterically shielded than the closer Li^+ ions and therefore are able to form stable solvation structures not predicted by the thermodynamic calculations. The thermodynamic analysis could be modified to attempt to replicate this but, with so many possible initial configurations, that task would be highly non trivial. The cause of this less bound or ordered state in the AIMD versus the thermodynamic calculations could be caused by the differences in the methods. The thermodynamic calculations will find the global lowest free energy state with a given initial configuration. The AIMD simulations will take the given input and explore the time progression of the system. Since the initial input is probably not at a low energy configuration, the system will approach lower energy states as it approaches equilibrium. Perhaps the system moving from an initial to an equilibrium state will cause this less bounded state.

Overall with a combination of dynamics and thermodynamics, the state of neutral Li_2PS species in a simplified electrolyte was determined. This better fundamental understanding and knowledge provides a great starting point for further calculations and investigation into the soluble long chain PS species.

Characterization of Polysulfide anionic species in Simple Electrolyte

Dynamics of LiS^-_6, LiS^-_8 Closed, LiS^-_8 Linear, S6, S^{-2}_8 Closed, and S^{-2}_8 Linear

As discussed earlier in the AIMD of neutral Li_2 polysulfide species, no separation of Li^+ and polysulfide was observed. Though this dissociation wasn't observed, the behavior of anionic or dianionic PSs without Li^+ ions are of great interest in order to understand the interactions of just the S atoms with the solvent, instead of the Li^+ bonded to S atoms with the solvent. The behavior of anionic PS species in the electrolyte is of great interest because if they are anionic in solution then the electric field present in the battery will cause an additional transport mechanism to move negatively charged species to the anode [35, 58] .

AIMD simulations for the LiS^-_6, LiS^-_8 Closed, LiS^-_8 Linear, S_6, S^{-2}_8 Closed, and S^{-2}_8 Linear species with DME and DOL were set following the same methodology used for the neutral Li_2 PS. The only changes made were the removal of 1 or 2 Li^+ ions and changing the overall charge of the cell to match. To have electroneutrality in the simulation cell, the VASP algorithm introduces a background charge of the opposite sign. The introduction of this background charge can have effects on the geometry of the system do to artifacts created by the correction. However as we show later, the structure of the anionic polysulfide's structure from periodic VASP simulations compared to the non-periodic Gaussian simulation's structure are similar indicating significant effects were not observed.

Snapshots of the anionic PS species with one Li^+ after 15 ps of simulation time are shown in Figure S14. From the AIMD trajectory analysis, it is found that the single Li^+ ions in the monoanions interact with the solvent molecules in the same way as if there were two Li^+ ions near the PS. In the cases of LiS^-_6 and LiS^-_8 closed, the Li^+ ion changes position to become centered directly in between the two end sulfur atoms instead of centered above or below. The solvent molecules also seem to interact with the PS anion in a different configuration than they would for the Li^+ ion. Their interaction can be explained by the partial charge analysis for the single anion species, Figure S15.

The electronic structure of the lithium PSs with overall charge of -1 is very similar to the neutral species. The charges are almost identical for the LiS^-_6 and LiS^-_8 closed molecules since they can share the Li^+ ion. The charge is more spread out amongst the S atoms on the anionic side for the LiS^-_8 linear molecule.

As described earlier, the solvent molecules should interact with the negatively charged S atoms differently than if they were interacting with Li^+ ions. From the AIMD, instead of the oxygen being the closely coordinating atom, the DME and DOL molecules are arranged such that their hydrogen atoms face the negatively charged anionic portion of the Li polysulfide. The RDFs for the LiS^-_8 Linear with DME and DOL is displayed in Figure 7. The corresponding RDF's for other systems are found in Figure S16.

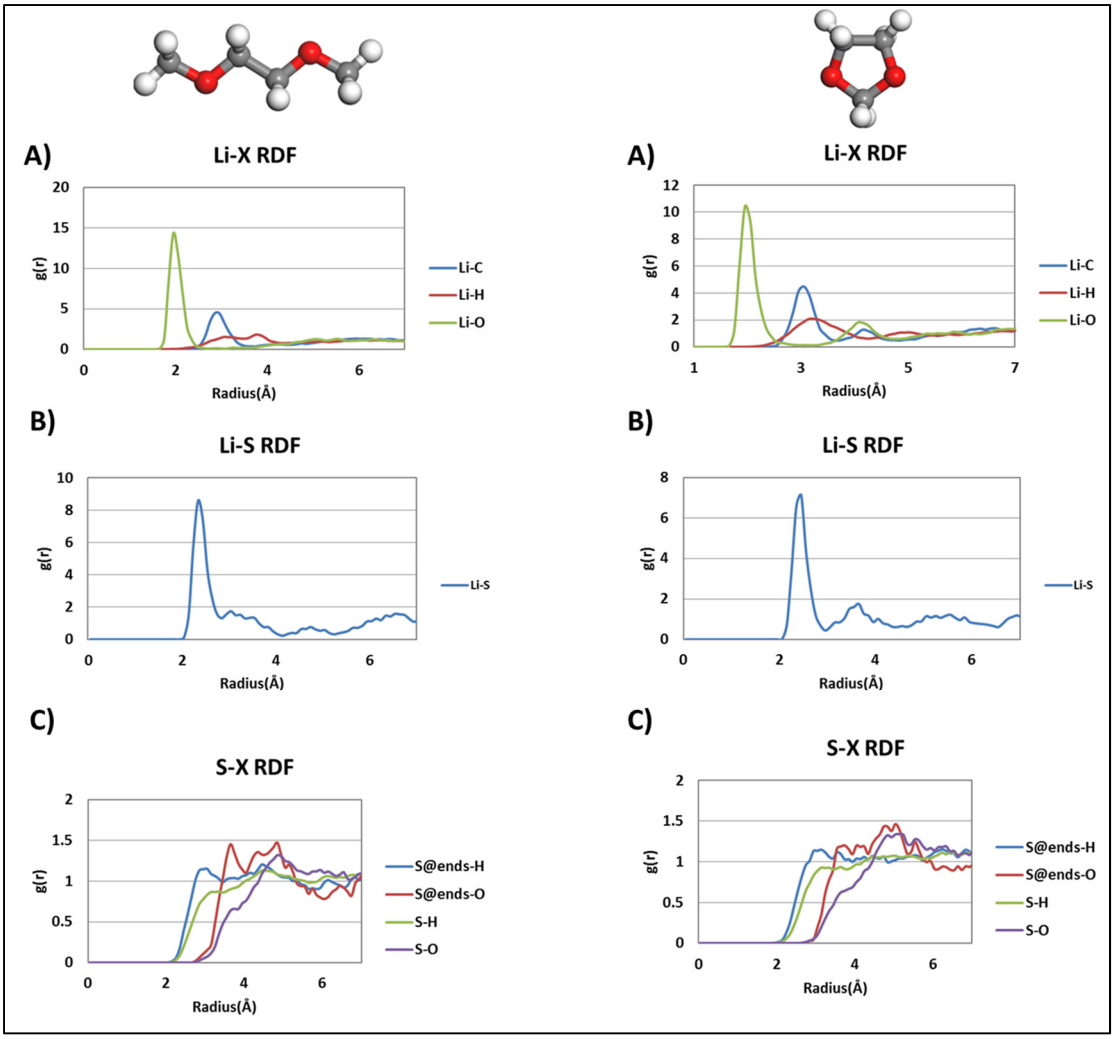

Figure 7: RDFs of the LiS^-_8 Linear interacting with the solvent; A) Li-X, B) Li-S , C) S-X RDF for DME (top) and DOL (bottom)

The RDFs look very similar to those for the neutral Li_2 polysulfide species, but there are several key differences. The Li-X RDF is practically identical to those in Figure 2. This is expected since taking away one Li^+ ion shouldn't change the nature of Li^+ ion – ether solvent interactions. The Li-S RDF also is very similar to the prior analysis for the neutral species because the Li^+ ion still remains closely bound to the PS. Just as with the neutral species, the remaining Li^+ does not detach from the PS. Ion pair dissociation was not observed in these simulations.

Unlike the previously considered interactions, the S-X RDFs are different between the Li and Li_2PS species. The peak for the S-H interactions with the end sulfur atoms is larger and the Li-O interactions with end S atoms are smaller. These both can be explained by the fact that on the anionic end of the molecule, H is coordinating with S instead of O. Therefore, the size of the S-H peak increases and the size of the S-O peak decreases.

Snapshots of the dianionic PS species after 15 ps of simulation time are shown in Figure S17. As identified in the previous case, the solvent molecules adopt configurations so that their hydrogen molecules can coordinate the sulfur atoms. The similarity can be described by the electronic structure of the PS species without any Li^+ ions (Figure S18).

The partial charges of the PS species do not change much with the presence or lack of Li^+ ions. The end S atoms for the dianion have similar charge to the end S atom without the Li^+ of the monoanion. Since the charge is similar for these atoms, the solvent molecules configuration near these atoms should be similar for the monoanion and dianion PS species. Though the electronic distribution stays relatively constant, the conformation of the PS itself does change. Without Li^+ ions to interact with the negatively charged polysulfide, the S^{2-}_8 closed molecule looks very similar to the S^{2-}_8 linear molecule. This change in conformation is to minimize the repulsive energy between the highly negatively charged ends of the polysulfide species.

Since the partial charges are similar to the other systems, the solvation occurs in a similar fashion. The RDF's for these systems are displayed in Figure 8. Corresponding RDFs for other PSs can be found in Figure S25.

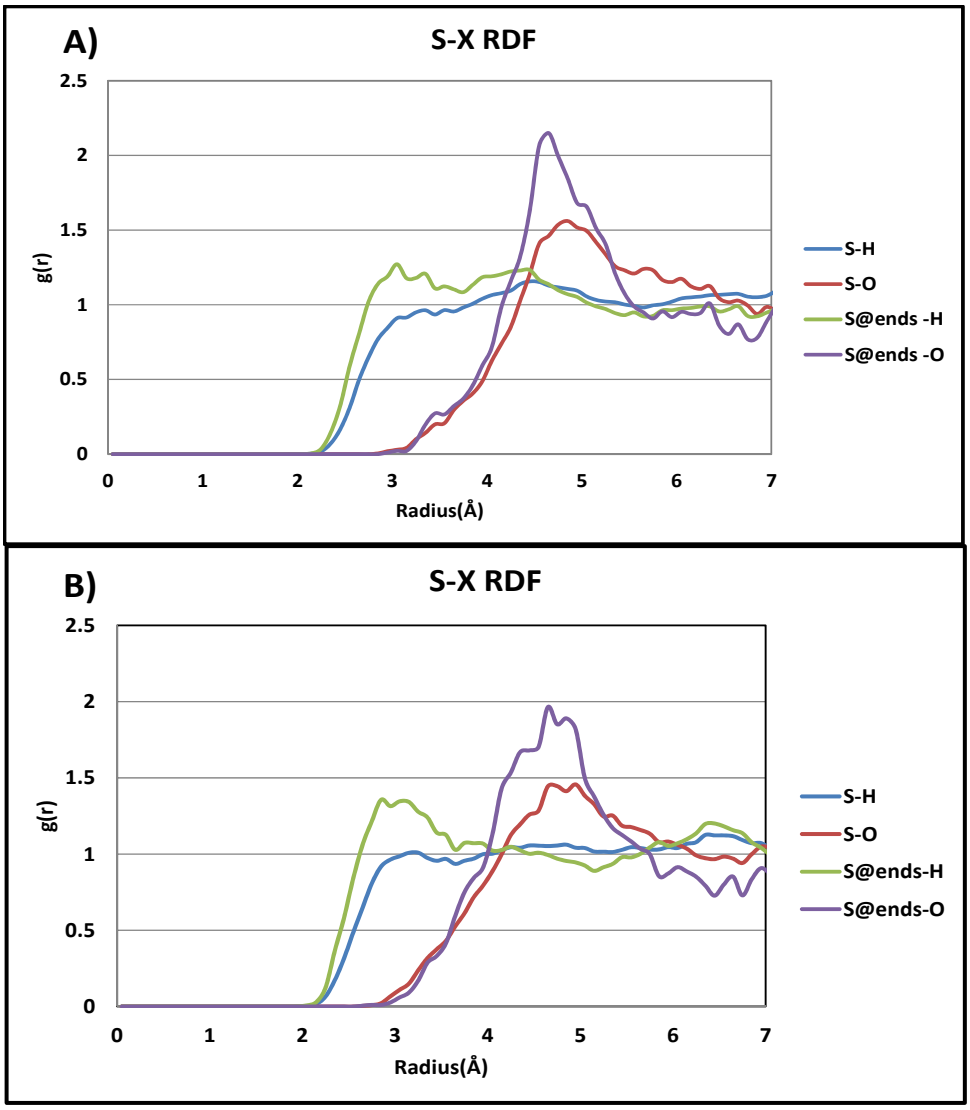

Figure 8: S^{-2}_8 Linear S-X RDF from the interactions with A) DME and B) DOL

As before, there is an actual peak for the end S atoms interactions with hydrogen because of coordination with the most negatively charged atoms. The peak for the oxygen and end sulfur atoms interactions is due to the hydrogen coordination and the molecular structure of the solvent.

The solvents interact in two different ways with the PS species. If the PSs exist as ion pairs with Li^+ ion then the main interaction is the oxygen atom in the solvent molecule coordinating with the ion. If the PSs exist as dianions without being bound to any Li^+ ions then the solvent will coordinate the end atoms of the PS species with their hydrogen atoms.

Thermodynamics of ion pair dissociation

The dynamics investigated the behavior of the important anionic PS species under the assumption that the anionic species were present in the electrolyte. From the simulations on

neutral Li_2 and anionic Li polysulfide species, the ion pair separation into the negatively charged polysulfide and the positively charged lithium ion was never observed. Therefore, ion pair dissociation thermodynamic calculations were done based on the stable solvation structures of neutral PS species previously identified (Figure S19).

If the $\Delta G_{dissociation}$ is negative, then the formation of an anionic Li polysulfide will be favored. The results of the calculation for the dissociation of 1 and 2 Li^+ ions can be found in Table 3. Example calculations specific to Li_2S_6 with DME are shown in Table 4.

Table 3: Solvation structures that thermodynamically favor ionic dissociation obtained from Hybrid PBE/6-311++G(d,p)/SMD. Labels of the structures correspond to Figure S7-S12.

Structures that favor Ionic Dissociation		
DME	**1st Li^+ ion**	**2nd Li^+ ion**
Li_2S_6	N/A	N/A
Li_2S_8 Closed	M, J	N/A
Li_2S_8 Linear	S,J,Z,T,M,U,AB	N/A
DOL		
Li_2S_6	N/A	N/A
Li_2S_8 Closed	N/A	N/A
Li_2S_8 Linear	N/A	N/A

Table 4: Li_2S_6 DME ion pair dissociation calculations obtained from Hybrid PBE/6-311++G(d,p)/SMD. Labels of the structures correpsond to Figure S7.

1st Li^+ ion		
Original Structure	**$\Delta G_{Dissociation}$ (kcal/mol)**	**Li^+ Solvation Structure**
B	22.42	**B**
N	17.27	**G**
C	25.05	**B**
I	12.11	**G**
I	26.75	**I**
O	20.29	**G**
2nd Li^+ ion		
B	22.42	**A**
N	17.27	**A**
C	25.05	**B**
I	12.11	**B**

I	26.75	**G**
O	20.29	**G**

Out of all the different systems tested, only the Li_2S_8 closed and Li_2S_8 linear configurations with DME had structures that favored dissociation of a single Li^+. Of those structures, none of them thermodynamically favored the dissociation of the 2nd Li^+. The Li_2S_8 linear configuration has more structures that favored dissociation compared to the closed configuration. One reason is that for the Li_2S_8 linear molecule, the polysulfide itself is already oriented to minimize any repulsive interactions from the sulfur with itself. Another reason is that for the linear conformation more solvent coordination is possible since the Li^+ ions are less shielded than in the closed conformation.

The results for the thermodynamics of the Li_2PS ion pair dissociation indicate that *dissociation is not favored* in the majority of the cases. If this is the case, then the PS would exist as an overall neutral species with 2 Li^+ ions bound to the dianionic PS in the electrolyte. The diffusion of the PS species for the PS shuttle effect would occur via concentration gradient driven mass transfer without extra effects from the electric field. Another possibility is that the model that was used for those calculations was too simple.

For the original dissociation calculation model, the only explicit molecules that were included were those coordinating Li^+ ions. No solvent molecules were included that were coordinating the anionic portion of the molecules for the total energy of the products calculation. One way to increase the complexity of the dissociation thermodynamic calculations would to be to include the solvent interactions with the sulfur atoms. Before those calculations can be completed, the thermodynamically favorable solvation structures for the anionic (1 Li^+) and dianionic (0 Li^+) must be known. Figure S20 shows the methodology used which is very similar to the solvation diagrams discussed earlier for DME and DOL. The structures that were tested are displayed in Figure S21 and Figure S22. These structures can be compared to those shown in Figures S15 and S18 which are the corresponding PS anions but from the VASP simulations. As discussed earlier, the inclusion of a neutralizing background charge is required for periodic simulations to be run successfully but the introduction of a charge may affect the system. When comparing the structures of the PS anions between periodic and non-periodic simulations, very few differences are observed. This indicates that the introduction of the background charge doesn't change significantly the structure of the PS and LiPS anions.

The structures for DME and DOL and their positions relative to the polysulfide were based on structures seen in the AIMD simulations of these same species. Unlike the solvation structure simulations with the Li^+, all of the ΔG's were positive (Table S1).

This means that the most stable structure for the polysulfide by itself would be one with *no solvent molecules*. This result is quite interesting since the solvent molecules do interact with the polysulfides as seen in the dynamics simulations. Single point calculations were done on these anion solvation structures to calculate the interaction energy between the solvent molecule and the polysulfide species. All the interaction energies were strongly positive which means that the interactions were repulsive. The solvent configurations with the hydrogen atoms oriented towards the polysulfide are less repulsive but still not attractive. The ether solvent molecules do not want to be too close to the polysulfide, but if they are near each other, the solvent will adopt a configuration to minimize that unfavorable energy. Since this interaction is repulsive, that implies that the polysulfide anion is not soluble in the electrolyte. In the past it was proposed that if the charges in the polysulfide anion rearranged, then solvent molecules would interact with the polysulfide attractively [9]. However, this rearrangement was not observed for any of the studied systems.

Another way to modify the dissociation calculations is the inclusion of electric field effects. It is known that electric fields will affect the dissociation of ion pairs and have other effects on chemical systems [59]. Electric field effects were not included in the quantum chemical calculations. But these effects were estimated as discussed below.

This analysis leads to the conclusion that the polysulfide may not be an anion in the bulk electrolyte solution. This does not mean that the polysulfide species is insoluble. Instead, the polysulfide is soluble in the electrolyte as an overall neutrally charged polysulfide anion with 2 Li^+. The solvation of these PS species could be imagined like a "tugboat". The sulfur atoms of the polysulfide interact repulsively with the solvent molecules but they interact closely with the Li^+ ions. The solvent molecules attractively and strongly interact with the Li^+ ions. Therefore, the solvent molecules could pull the Li^+ ions which would pull the polysulfide in turn. This interaction provides a potential mechanism that would solvate the polysulfide species.

Thus, the PS shuttle effect wouldn't occur via anionic polysulfides but instead with neutral lithiated polysulfide species. The shuttle effect would still occur but the driving force would be *purely concentration gradient* instead of a combination of that with a potential gradient driving force. If the electric field is strong enough, then it might cause the results to favor dissociation of neutral Li_2PS (still would favor $LiPS^-$ over PS^{2-}). Then the potential would have an effect on the migration of polysulfides. The effect of the electric field on the thermodynamic equilibrium constant can be estimated with a simple formula from Onsager [59]. The formula, parameters and example calculation are shown in the supporting information. Based on the conservatively estimated parameters, the electric field causes the $\Delta G_{dissociation}$ to decrease around 1 kcal/mol. This indicates that the electric field will have some effect on the dissociation but not a large one.

If this model is accurate, then increases in ionic conductivity would lead to potential increases in the polysulfide shuttle effect. Peled found that when using DOL that has a much higher ionic conductivity than THF, but also found a decrease in sulfur utilization which could be caused by

the shuttle phenomena [26]. Increasing concentration of lithium salts has been found to decrease polysulfide solubility. This phenomenon can be attributed to a decrease in free solvent molecules as the salt concentration increases. With less free solvent molecules, the ionic conductivity of Li^+ can decrease and therefore polysulfide solubility decreases.[23, 34, 58, 60]. High lithium salt concentration can also help with performance issues related to the negative electrode like SEI formation and dendrite growth restriction [60].

Characterization of Li_2S_6, Li_2S_8 Closed, Li_2S_8 Linear in Electrolyte with extra Li^+ ions

After studying different polysulfide species in varying degrees of coordination with Li^+ ions, the model for the electrolyte was increased in complexity by the inclusion of more Li^+ ions in the electrolyte. During Li-S battery operation, the electrolyte is expected to have a higher concentration of Li^+ ions that are being moved toward the cathode during discharge have the potential to interact with the dissolved Li_2PS species. AIMD simulations were run for the same systems as before but also including 1,2, and 3 extra Li^+ ions. Snapshots of these simulations after 15 ps are shown in Figure S23.The interactions between the different atomic species in these simulations should follow the same trends and mechanisms as described earlier. The RDF's of the Li-X interactions are displayed in Figure 9 for Li_2S_8 Linear with DME and DOL solvents. Corresponding RDFs for other systems can be found in Figure S24.

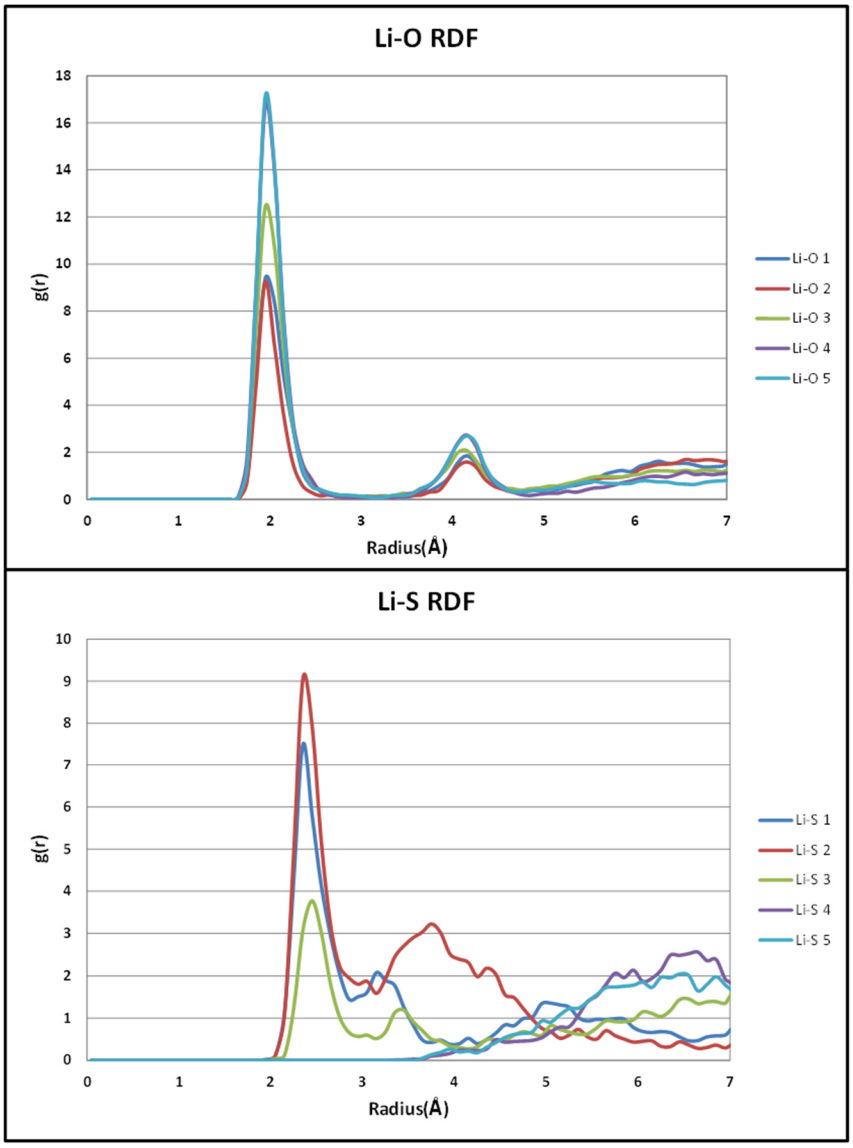

Figure 9: Li_2S_8 Linear with DME with 3 extra Li^+

Based on the initial configurations of these simulations, the Li^+ ions can either be bound to the polysulfide or free in solution. The Li-S RDF for a free Li^+ should be peakless since it isn't coordinating with the sulfur atoms. On the other hand, a free Li^+ should have a stronger oxygen peak since more solvent molecules can fit around it due to lack of shielding by the polysulfide molecule.

These observations were held to be true with a couple of interesting deviations. Most of the Li^+ ions stayed in the same state as their initial configuration, bound or free. However in some of the cases, the Li^+ ions are best described as being somewhere in a slightly bound state between those two states. This can be clearly visualized in the RDFs because the intermediate peaks will be noticeably in between the RDF peaks for a perfectly free and a perfectly bound Li^+ ion. This observation allows for a more loosely defined lithium polysulfide cluster like structure, with

possibilities of having polysulfide species with more than just two Li^+ ions interacting. However, when an extra Li^+ ion starts coordinating with the neutral Li_2 polysulfide species, one of the bound Li^+ becomes more weakly bound.

These simulations indicate that if free Li^+ ions are present in the solution; the polysulfide would closely interact with it especially if the polysulfide exists without being closely bound to any Li^+ ions. Since the polysulfide has these interactions, it is possible to imagine that multiple polysulfides could exist as clusters in solution of multiple Li^+ and polysulfide anions. This phenomena has been suggested and possibly observed before [4].

Conclusions

The behavior, structure, and state of long chain polysulfide species in Li-S battery electrolyte were investigated with first principles methods. The behavior and structure of polysulfides with different levels of Li^+ coordination (2 Li^+, 1 Li^+, 0 Li^+) in the presence of DME and DOL were determined with AIMD and DFT calculations.

The thermodynamically favorable 1st solvation shell for Li^+ ion in DME and DOL was determined as well as the stable 1st solvation shell for neutral Li_2 polysulfide species. The solvent molecules interacted almost solely with the Li^+ ions with little differences between DME and DOL solvation. Throughout all of the AIMD simulations that were run, ion pair dissociation of the polysulfide species and Li^+ ions was never observed. Free energy calculations also demonstrated that only very few of the thermodynamically stable solvation structures would favor dissociation. These results indicated that perhaps the dissolved polysulfide taking part in the shuttle effect may be a neutral species. Simulations with extra Li^+ indicated that polysulfides would coordinate with more than just 2 Li^+ ions creating more complicated structures. Multiple Li^+ coordination with polysulfides may give rise to the idea of polysulfide cluster formation with multiple polysulfides and Li^+ ions.

Future work will explore more complicated electrolyte models including lithium salts and additives as well as screening more electrolyte compositions. The effects of the electrified interface will also be explored due to its great importance in the initiation of the polysulfide shuttle phenomenon.

Supporting Information: Molecular structures (S1); radial distribution functions (S2-I and II; S16-I and II, S24 I, II, III; S25 I and II); Bader charges (S3, S15, S18); solvation structures (S4, S5, S7 to S12, S21, S22,); thermodynamically favored solvation structures and pathways (S6); time evolution of coordination number (S13-I and II); Snapshots from AIMD (S14, S17, S23-I, II, III;); schematic of methodology for dissociation analysis (S19, S20); ΔG of solvation (Table S1, S2, S4 to S9); Total energies in solvation models (Table S3); ΔG of dissociation (Tables S10 to S22); Electric Field effect estimation. This information is available free of charge via the Internet at http://pubs.acs.org.

Acknowledgements: This work was supported by the Assistant Secretary for Energy Efficiency and Renewable Energy, Office of Vehicle Technologies of the U.S. Department of Energy under Contract No. DE-EE0006832 under the Advanced Battery Materials Research (BMR) Program. EPK acknowledges the National Science Foundation for a Graduate Research Fellowship. Supercomputer resources from Texas A&M University High Performance Computer Center and Texas Advanced Computing Center (TACC) are gratefully acknowledged.

References

1. Pang, Q.; Liang, X.; Kwok, C. Y.; Nazar, L. F., Advances in Lithium–Sulfur Batteries Based on Multifunctional Cathodes and Electrolytes. *Nat. Mater.* **2016,** *1*, 16132.
2. Xiong, S.; Xie, K.; Diao, Y.; Hong, X., Characterization of the Solid Electrolyte Interphase on Lithium Anode for Preventing the Shuttle Mechanism in Lithium–Sulfur Batteries. *J. Power Sources* **2014,** *246*, 840-845.
3. Weng, W.; Pol, V. G.; Amine, K., Ultrasound Assisted Design of Sulfur/Carbon Cathodes with Partially Fluorinated Ether Electrolytes for Highly Efficient Li/S Batteries. *Adv. Mater.* **2013,** *25* (11), 1608-1615.
4. Diao, Y.; Xie, K.; Xiong, S.; Hong, X., Analysis of Polysulfide Dissolved in Electrolyte in Discharge-Charge Process of Li-S Battery. *J. Electrochem. Soc.* **2012,** *159* (4), A421-A425.
5. Abraham, K. M., Rechargeable Batteries for the 300-Mile Electric Vehicle and Beyond. *ECS Trans* **2012,** *41* (31), 27-34.
6. Ji, X.; Nazar, L. F., Advances in Li-S Batteries. *J. Mater. Chem.* **2010,** *20* (44), 9821-9826.
7. Diao, Y.; Xie, K.; Xiong, S.; Hong, X., Shuttle Phenomenon – The Irreversible Oxidation Mechanism of Sulfur Active Material in Li–S Battery. *J. Power Sources* **2013,** *235*, 181-186.
8. Kang, W.; Deng, N.; Ju, J.; Li, Q.; Wu, D.; Ma, X.; Li, L.; Naebe, M.; Cheng, B., A Review of Recent Developments in Rechargeable Lithium-Sulfur Batteries. *Nanoscale* **2016,** *8* (37), 16541-16588.
9. Rauh, R. D.; Shuker, F. S.; Marston, J. M.; Brummer, S. B., Formation of Lithium Polysulfides in Aprotic Media. *J. Inorg. Nucl. Chem.* **1977,** *39* (10), 1761-1766.
10. Choi, J.-W.; Kim, J.-K.; Cheruvally, G.; Ahn, J.-H.; Ahn, H.-J.; Kim, K.-W., Rechargeable Lithium/Sulfur Battery With Suitable Mixed Liquid Electrolytes. *Electrochim. Acta* **2007,** *52* (5), 2075-2082.
11. Cresce, A. V.; Russell, S. M.; Borodin, O.; Allen, J. A.; Schroeder, M. A.; Dai, M.; Peng, J.; Gobet, M. P.; Greenbaum, S. G.; Rogers, R. E.; Xu, K., Solvation Behavior of Carbonate-Based Electrolytes in Sodium Ion Batteries. *Phys. Chem. Chem. Phys.* **2017,** *19* (1), 574-586.
12. Liang, X.; Hart, C.; Pang, Q.; Garsuch, A.; Weiss, T.; Nazar, L. F., A Highly Efficient Polysulfide Mediator for Lithium–Sulfur Batteries. *Nat. Commun.* **2015,** *6*, 5682.
13. Li, X.; Zhao, K.; Zhang, L.; Ding, Z.; Hu, K., MoS2-Decorated Coaxial Nanocable Carbon Aerogel Composites as Cathode Materials for High Performance Lithium-Sulfur Batteries. *J. Alloys Compd.* **2017,** *692*, 40-48.
14. Kamphaus, E. P.; Balbuena, P. B., Long-Chain Polysulfide Retention at the Cathode of Li–S Batteries. *J. Phys. Chem. C* **2016,** *120* (8), 4296-4305.
15. Pang, Q.; Kundu, D.; Cuisinier, M.; Nazar, L. F., Surface-Enhanced Redox Chemistry of Polysulphides on a Metallic and Polar host for Lithium-Sulphur Batteries. *Nat. Commun.* **2014,** *5*, 4759.

16. He, G.; Mandlmeier, B.; Schuster, J.; Nazar, L. F.; Bein, T., Bimodal Mesoporous Carbon Nanofibers with High Porosity: Freestanding and Embedded in Membranes for Lithium–Sulfur Batteries. *Chem. Mater.* **2014,** *26* (13), 3879-3886.
17. Pascal, T. A.; Wujcik, K. H.; Wang, D. R.; Balsara, N. P.; Prendergast, D., Thermodynamic Origins of the Solvent-Dependent Stability of Lithium Polysulfides from First Principles. *Phys. Chem. Chem. Phys.* **2017,** *19* (2), 1441-1448.
18. Gao, J.; Lowe, M. A.; Kiya, Y.; Abruña, H. D., Effects of Liquid Electrolytes on the Charge–Discharge Performance of Rechargeable Lithium/Sulfur Batteries: Electrochemical and in-Situ X-ray Absorption Spectroscopic Studies. *J. Phys. Chem. C* **2011,** *115* (50), 25132-25137.
19. Park, J.-W.; Yamauchi, K.; Takashima, E.; Tachikawa, N.; Ueno, K.; Dokko, K.; Watanabe, M., Solvent Effect of Room Temperature Ionic Liquids on Electrochemical Reactions in Lithium–Sulfur Batteries. *J. Phys. Chem. C* **2013,** *117* (9), 4431-4440.
20. Shakourian-Fard, M.; Kamath, G.; Sankaranarayanan, S. K. R. S., Evaluating the Free Energies of Solvation and Electronic Structures of Lithium-Ion Battery Electrolytes. *ChemPhysChem* **2016,** *17* (18), 2916-2930.
21. Rauh, R. D.; Abraham, K. M.; Pearson, G. F.; Surprenant, J. K.; Brummer, S. B., A Lithium/Dissolved Sulfur Battery with an Organic Electrolyte. *J. Electrochem. Soc.* **1979,** *126* (4), 523-527.
22. Yamin, H.; Penciner, J.; Gorenshtain, A.; Elam, M.; Peled, E., The Electrochemical Behavior of Polysulfides in Tetrahydrofuran. *J. Power Sources* **1985,** *14* (1), 129-134.
23. Cuisinier, M.; Cabelguen, P. E.; Adams, B. D.; Garsuch, A.; Balasubramanian, M.; Nazar, L. F., Unique Behaviour of Nonsolvents for Polysulphides in Lithium-Sulphur Batteries. *Energy & Environmental Science* **2014,** *7* (8), 2697-2705.
24. Yamada, Y.; Furukawa, K.; Sodeyama, K.; Kikuchi, K.; Yaegashi, M.; Tateyama, Y.; Yamada, A., Unusual Stability of Acetonitrile-Based Superconcentrated Electrolytes for Fast-Charging Lithium-Ion Batteries. *J. Am. Chem. Soc.* **2014,** *136* (13), 5039-5046.
25. Henderson, W. A., Glyme−Lithium Salt Phase Behavior. *J. Phys. Chem. B* **2006,** *110* (26), 13177-13183.
26. Peled, E.; Sternberg, Y.; Gorenshtein, A.; Lavi, Y., Lithium-Sulfur Battery: Evaluation of Dioxolane-Based Electrolytes. *J. Electrochem. Soc.* **1989,** *136* (6), 1621-1625.
27. Camacho-Forero, L. E.; Smith, T. W.; Balbuena, P. B., Effects of High and Low Salt Concentration in Electrolytes at Lithium–Metal Anode Surfaces. *J. Phys. Chem. C* **2017,** *121* (1), 182-194.
28. Hagen, M.; Hanselmann, D.; Ahlbrecht, K.; Maça, R.; Gerber, D.; Tübke, J., Lithium–Sulfur Cells: The Gap between the State-of-the-Art and the Requirements for High Energy Battery Cells. *Adv. Energy Mater.* **2015,** *5* (16), 1401986-n/a.
29. Cuisinier, M.; Hart, C.; Balasubramanian, M.; Garsuch, A.; Nazar, L. F., Radical or Not Radical: Revisiting Lithium–Sulfur Electrochemistry in Nonaqueous Electrolytes. *Adv. Energy Mater.* **2015,** *5* (16), 1401801-n/a.
30. Saqib, N.; Silva, C. J.; Maupin, C. M.; Porter, J. M., A Novel Optical Diagnostic for In Situ Measurements of Lithium Polysulfides in Battery Electrolytes. *Appl. Spectrosc. 0* (0), 0003702816684638.
31. Barchasz, C.; Molton, F.; Duboc, C.; Leprêtre, J.-C.; Patoux, S.; Alloin, F., Lithium/Sulfur Cell Discharge Mechanism: An Original Approach for Intermediate Species Identification. *Anal. Chem.* **2012,** *84* (9), 3973-3980.

32. Cuisinier, M.; Cabelguen, P.-E.; Evers, S.; He, G.; Kolbeck, M.; Garsuch, A.; Bolin, T.; Balasubramanian, M.; Nazar, L. F., Sulfur Speciation in Li–S Batteries Determined by Operando X-ray Absorption Spectroscopy. *J. Phys. Chem. Lett.* **2013,** *4* (19), 3227-3232.
33. Hannauer, J.; Scheers, J.; Fullenwarth, J.; Fraisse, B.; Stievano, L.; Johansson, P., The Quest for Polysulfides in Lithium–Sulfur Battery Electrolytes: An Operando Confocal Raman Spectroscopy Study. *ChemPhysChem* **2015,** *16* (13), 2755-2759.
34. Dokko, K.; Tachikawa, N.; Yamauchi, K.; Tsuchiya, M.; Yamazaki, A.; Takashima, E.; Park, J.-W.; Ueno, K.; Seki, S.; Serizawa, N.; Watanabe, M., Solvate Ionic Liquid Electrolyte for Li–S Batteries. *J. Electrochem. Soc.* **2013,** *160* (8), A1304-A1310.
35. Kumaresan, K.; Mikhaylik, Y.; White, R. E., A Mathematical Model for a Lithium–Sulfur Cell. *J. Electrochem. Soc.* **2008,** *155* (8), A576-A582.
36. Camacho-Forero, L. E.; Smith, T. W.; Bertolini, S.; Balbuena, P. B., Reactivity at the Lithium–Metal Anode Surface of Lithium–Sulfur Batteries. *J. Phys. Chem. C* **2015,** *119* (48), 26828-26839.
37. Rajput, N. N.; Murugesan, V.; Shin, Y.; Han, K. S.; Lau, K. C.; Chen, J.; Liu, J.; Curtiss, L. A.; Mueller, K. T.; Persson, K. A., Elucidating the Solvation Structure and Dynamics of Lithium Polysulfides Resulting from Competitive Salt and Solvent Interactions. *Chem. Mater.* **2017,** *29* (8), 3375-3379.
38. Kresse, G.; Furthmüller, J., Efficiency of Ab-Initio Total Energy Calculations for Metals and Semiconductors Using a Plane-Wave Basis Set. *Comput. Mater. Sci* **1996,** *6* (1), 15-50.
39. Kresse, G.; Hafner, J., Ab Initio Molecular Dynamics for Liquid Metals. *Phys. Rev. B* **1993,** *47* (1), 558-561.
40. Kresse, G.; Hafner, J., Ab Initio Molecular-Dynamics Simulation of the Liquid-Metal–Amorphous-Semiconductor Transition in Germanium. *Phys. Rev. B* **1994,** *49* (20), 14251-14269.
41. Blochl, P. E., Projector Augmented-Wave Method. *Phys. Rev. B* **1994,** *50* (24), 17953-17979.
42. Kresse, G.; Joubert, D., From ultrasoft pseudopotentials to the projector augmented-wave method. *Phys. Rev. B* **1999,** *59* (3), 1758-1775.
43. Perdew, J. P.; Burke, K.; Ernzerhof, M., Generalized Gradient Approximation Made Simple. *Phys. Rev. Lett.* **1996,** *77* (18), 3865-3868.
44. Monkhorst, H. J.; Pack, J. D., Special Points for Brillouin-Zone Integrations. *Phys. Rev. B* **1976,** *13* (12), 5188-5192.
45. de Leeuw, S. W.; Perram, J. W.; Smith, E. R., Simulation of electrostatic systems in periodic boundary conditions. I. Lattice sums and dielectric constants. *Proc. R. Soc. Lond.* **1980,** *A 373*, 27-56.
46. Rappe, A. K.; Casewit, C. J.; Colwell, K. S.; Goddard, W. A.; Skiff, W. M., UFF, a full periodic table force field for molecular mechanics and molecular dynamics simulations. *J. Am. Chem. Soc.* **1992,** *114*, 10024-10035.
47. Tang, W.; Sanville, E.; Henkelman, G., A Grid-Based Bader Analysis Algorithm Without Lattice Bias. *J. Phys. Condens. Matter* **2009,** *21* (8), 084204.
48. Sanville, E.; Kenny, S. D.; Smith, R.; Henkelman, G., Improved Grid-Based Algorithm for Bader Charge Allocation. *J. Comput. Chem.* **2007,** *28* (5), 899-908.
49. Henkelman, G.; Arnaldsson, A.; Jónsson, H., A fast and Robust Algorithm for Bader Decomposition of Charge Density. *Comput. Mater. Sci* **2006,** *36* (3), 354-360.
50. Humphrey, W.; Dalke, A.; Schulten, K., VMD: Visual molecular dynamics. *J. Mol. Graph. Model.* **1996,** *14* (1), 33-38.

51. Frisch, M. J.; Trucks, G. W.; Schlegel, H. B.; Scuseria, G. E.; Robb, M. A.; Cheeseman, J. R.; Scalmani, G.; Barone, V.; Mennucci, B.; Petersson, G. A.; Al., E. *Gaussian 09, Revision B.01*, Wallingford CT, 2009.
52. McQuarrie, D. A., *Statistical Mechanics*. University Science Books: 2000.
53. Ernzerhof, M.; Scuseria, G. E., Assessment of the Perdew–Burke–Ernzerhof Exchange-Correlation Functional. *J. Chem. Phys.* **1999,** *110* (11), 5029-5036.
54. Perdew, J. P.; Chevary, J. A.; Vosko, S. H.; Jackson, K. A.; Pederson, M. R.; Singh, D. J.; Fiolhais, C., Atoms, Molecules, Solids, and Surfaces: Applications of the Generalized Gradient Approximation for Exchange and Correlation. *Phys. Rev. B* **1992,** *46* (11), 6671-6687.
55. Cramer, C. J.; Truhlar, D. G., A Universal Approach to Solvation Modeling. *Acc. Chem. Res.* **2008,** *41* (6), 760-768.
56. Chapman, N.; Borodin, O.; Yoon, T.; Nguyen, C. C.; Lucht, B. L., Spectroscopic and Density Functional Theory Characterization of Common Lithium Salt Solvates in Carbonate Electrolytes for Lithium Batteries. *J. Phys. Chem. C* **2017,** *121* (4), 2135-2148.
57. Olsher, U.; Izatt, R. M.; Bradshaw, J. S.; Dalley, N. K., Coordination Chemistry of Lithium Ion: A Crystal and Molecular Structure Review. *Chem. Rev.* **1991,** *91* (2), 137-164.
58. Mikhaylik, Y. V.; Akridge, J. R., Polysulfide Shuttle Study in the Li/S Battery System. *J. Electrochem. Soc.* **2004,** *151* (11), A1969-A1976.
59. Neumann, E., *Principles of Electric Field Effects in Chemical and Biological Systems*. 1981; Vol. 4.
60. Qian, J.; Henderson, W. A.; Xu, W.; Bhattacharya, P.; Engelhard, M.; Borodin, O.; Zhang, J.-G., High Rate and Stable Cycling of Lithium Metal Anode. *Nat. Commun.* **2015,** *6*, 6362.

Table of Contents Graphic